

E. Lerche, D. Van Eester, J. Ongena, M.-L. Mayoral, T. Johnson, T. Hellsten,  
R. Bilato, A. Czarnecka, R. Dumont, C. Giroud, P. Jacquet, V. Kiptily,  
A. Krasilnikov, M. Maslov, V. Vdovin and JET EFDA contributors

# ICRF Scenarios for ITER's Half-Field Phase

# ICRF Scenarios for ITER's Half-Field Phase

E. Lerche<sup>1</sup>, D. Van Eester<sup>1</sup>, J. Ongena<sup>1</sup>, M.-L. Mayoral<sup>2</sup>, T. Johnson<sup>3</sup>, T. Hellsten<sup>3</sup>,  
R. Bilato<sup>4</sup>, A. Czarnecka<sup>5</sup>, R. Dumont<sup>6</sup>, C. Giroud<sup>2</sup>, P. Jacquet<sup>2</sup>, V. Kiptily<sup>2</sup>,  
A. Krasilnikov<sup>7</sup>, M. Maslov<sup>8</sup>, V. Vdovin<sup>9</sup> and JET EFDA contributors\*

*JET-EFDA, Culham Science Centre, OX14 3DB, Abingdon, UK*

<sup>1</sup>*LPP-ERM/KMS, Association EURATOM-‘Belgian State’, TEC Partner, Brussels, Belgium*

<sup>2</sup>*EURATOM-CCFE Fusion Association, Culham Science Centre, OX14 3DB, Abingdon, OXON, UK*

<sup>3</sup>*Fusion Plasma Physics, Association EURATOM-VR, KTH, Stockholm, Sweden*

<sup>4</sup>*IPP(MPI)-EURATOM Association, Garching, Germany*

<sup>5</sup>*Institute of Plasma Physics and Laser Microfusion, Warsaw, Poland*

<sup>6</sup>*CEA(IRFM)-Euratom Association, Saint-Paul-lez-Durance, France*

<sup>7</sup>*SRC RF Troitsk Institute for Innovating and Fusion Research, Troitsk, Russia*

<sup>8</sup>*Centre de Recherches en Physique des Plasmas, Association EURATOM-Conf. Suisse, Lausanne, CH*

<sup>9</sup>*RNC Kurchatov Institute, Nuclear Fusion Institute, Moscow, Russia*

\* *See annex of F. Romanelli et al, “Overview of JET Results”,  
(23rd IAEA Fusion Energy Conference, Daejeon, Republic of Korea (2010)).*

Preprint of Paper to be submitted for publication in Proceedings of the  
19th Topical Conference on Radio Frequency Power in Plasmas,  
Newport, Rhode Island, USA  
(1st June 2011 - 3rd June 2011)

“This document is intended for publication in the open literature. It is made available on the understanding that it may not be further circulated and extracts or references may not be published prior to publication of the original when applicable, or without the consent of the Publications Officer, EFDA, Culham Science Centre, Abingdon, Oxon, OX14 3DB, UK.”

“Enquiries about Copyright and reproduction should be addressed to the Publications Officer, EFDA, Culham Science Centre, Abingdon, Oxon, OX14 3DB, UK.”

The contents of this preprint and all other JET EFDA Preprints and Conference Papers are available to view online free at [www.iop.org/Jet](http://www.iop.org/Jet). This site has full search facilities and e-mail alert options. The diagrams contained within the PDFs on this site are hyperlinked from the year 1996 onwards.



## ABSTRACT

The non-active operation phase of ITER will be done in H and  $4\text{He}$  plasmas at half the nominal magnetic field,  $B_0 = 2.65\text{T}$ . At this field and for the given frequency range of the ICRF system ( $f = 40\text{-}55\text{MHz}$ ), three ICRF heating scenarios are available a priori: (i) Fundamental ICRH of majority H plasmas at  $f \approx 40\text{MHz}$ , (ii) second harmonic ( $N=2$ )  $^3\text{He}$  ICRH in H plasmas at  $f \approx 53\text{MHz}$  and (iii) fundamental minority H heating in  $4\text{He}$  plasmas at  $f \approx 40\text{MHz}$ . While the latter is expected to perform well for not too large H concentrations, the heating scenarios available for the Hydrogen plasmas are less robust. Recent JET experiments performed in similar conditions to those expected in ITER's half-field phase confirmed the low performance of these two scenarios and numerical simulations have shown that the situation is not much improved in ITER, mainly because of the rather modest plasma temperature and density expected in its initial operation phase. A summary of the main experimental results obtained at JET followed by numerical predictions for ITER's half-field ICRF heating scenarios will be presented.

## INTRODUCTION

ITER will start its operation with Hydrogen and  $^4\text{He}$  plasmas at reduced magnetic field. At half the nominal field,  $B_0 = 2.65\text{T}$ , and with the auxiliary power currently foreseen to be available in this phase, 16.5MW off-axis Neutral Beam Injection (NBI), 15MW off-axis Electron Cyclotron Resonance Heating (ECRH) and 10MW on-axis Ion Cyclotron Resonance Heating (ICRH), most discharges are expected to be in L-mode and typical central densities of  $n_0 \approx 3.5 \times 10^{19} \text{ m}^{-3}$  and central temperatures of approximately  $T_i = 8\text{keV}$  and  $T_e = 10\text{keV}$  are estimated [1]. In these calculations, it was envisaged that 10MW of ICRF power would be sufficient for raising the ion and electron temperatures from  $T_i \approx T_e = 5\text{keV}$  to  $T_i = 8\text{keV}$  and  $T_e = 10\text{keV}$ , respectively, if central ICRF heating with equal power sharing between electrons and ions is considered. This is an optimistic assessment and assumes that all the power launched by the ICRF antenna is absorbed in the plasma (100% heating efficiency).

In Hydrogen plasmas and for the designed frequency range of the ICRF heating system in ITER ( $f = 40\text{-}55\text{MHz}$ ), fundamental ( $N=1$ ) ion cyclotron heating of H majority ions at  $f \approx 40\text{MHz}$  and 2<sup>nd</sup> harmonic ( $N=2$ ) ion cyclotron heating of  $^3\text{He}$  ions at  $f \approx 53\text{MHz}$  are possible scenarios for central ion heating at  $B_0 = 2.65\text{T}$ . However, both are characterized by poor ion absorption: The  $N=1$  H majority scenario suffers from the adverse polarization of the RF fields close to the ion cyclotron resonance layer of the majority H ions ('screening effect') whereas the  $N=2$   $^3\text{He}$  heating scheme requires a relatively large fraction of 'minority' ions to become efficient. Results of recent JET experiments [2] and preliminary numerical simulations of the ICRF heating scenarios for ITER's half-field Hydrogen phase [3,4] confirm that low single-pass power absorption with dominant fast wave electron heating will take place, and that high heating efficiencies (as those typically observed in fundamental ICRF minority heating) will be unlikely.

Although expected to be performing well at moderate Hydrogen concentrations, the *classical*  $N = 1$  H minority heating scheme to be used in the  $^4\text{He}$  plasma phase of ITER may become less efficient if the H concentration gets too large, as e.g. by H-pellet injection for ELM control in H-mode discharges. This well known effect was observed experimentally in many tokamak's [5,6] and was also confirmed numerically [7].

Given the fact that ITER will strongly rely on every MW of auxiliary heating power that can be injected into the plasma, numerical and experimental investigations aiming at testing and optimizing the performance of these ICRF scenarios are crucial for a successful operation of ITER in its early phase. In this paper, the main results from recent JET experiments focusing on the ICRF scenarios for ITER's half-field Hydrogen phase followed by preliminary numerical predictions of their performance in ITER conditions are presented. The simulations also include an example of the influence of the H concentration on the  $N = 1$  H minority scenario foreseen for the  $^4\text{He}$  plasma phase.

## SUMMARY OF JET EXPERIMENTS

The ICRF parameters of the half-field phase of ITER in H plasmas were closely reproduced in the JET experiments [2]: The  $N=1$  H majority heating scenario was studied at  $f = 42.5\text{MHz} / B_0 = 2.65\text{T}$  and the  $N = 2$   $^3\text{He}$  heating experiments were done at  $f = 51.5\text{MHz} / B_0 = 2.65\text{T}$ . In these conditions, the fundamental ion cyclotron resonance layer of the H ions and the 2<sup>nd</sup> harmonic ion cyclotron resonance of the  $^3\text{He}$  ions are both located near the plasma centre. The antenna phasing was dipole ( $k_{\parallel} \approx 6.5\text{m}^{-1}$ ) in both cases and up to 5.5MW of ICRF power was coupled to the plasma. Aside from the different ICRF settings and the dilution of the H plasmas with  $^3\text{He}$  in the  $N = 2$   $^3\text{He}$  heating pulses (no  $^3\text{He}$  was injected in the  $N = 1$  H heating discharges), the plasmas were similar in the two sessions. Both experiments were performed in L-mode and adopted a low triangularity plasma shape, with antenna - plasma (separatrix) distances around 9.5-11.0cm. Typical central densities of  $n_0 \approx 3 \times 10^{19}/\text{m}^3$  and central temperatures ranging from  $T_e = 2\text{-}4\text{keV}$ , depending on the NBI power applied ( $0 < P_{\text{NBI}} < 8\text{MW}$ ), were obtained in the discharges. Although the central densities of the JET experiments are comparable to those expected in the initial phase of ITER, both electron and ion temperatures are well below leading to a different collisional regime than the one expected in ITER. The experimental ICRF heating efficiencies ( $\eta = \text{power transferred to the bulk plasma} / \text{coupled power}$ ) for electrons and H ions obtained by analyzing, respectively, the electron cyclotron emission and charge-exchange signal responses to fast variations in the applied ICRF power [8] are depicted in Fig.1 for the fundamental H majority experiments (left) and for the 2<sup>nd</sup> harmonic  $^3\text{He}$  heating experiments (right). The prompt response of the electron temperature to the ICRF power variations confirm that in both scenarios the electron absorption is mainly due to direct fast wave Landau damping (ELD) and Transit Time Magnetic Pumping (TTMP) and not to collisional slowing-down of ICRF accelerated ions, as is usually the case in minority heating schemes. For the H majority case, the electrons absorb typically twice as much RF power as the ions and both absorptivities increase with the central plasma temperature, reaching a total heating efficiency of  $\eta \approx 0.4$  at  $T_{e0} = 2.5\text{keV}$ .

The slope of the heating efficiency of the ions is somewhat steeper than the one of the electrons, indicating that the ion cyclotron absorption of the H ions is privileged when increasing the bulk plasma temperature within the studied range. For the  $N = 2$   $^3\text{He}$  heating scenario, the dependence of the heating efficiency with the temperature was minor, but a clear enhancement of the ICRF absorption for higher  $^3\text{He}$  concentrations was observed. Note that it is the ion heating that is mainly improved at higher  $^3\text{He}$  concentrations and that the total heating efficiency reached at  $X[^3\text{He}] \approx 20\%$ , where the ion absorption exceeds that of the electrons, is similar to the one obtained for the H majority case ( $\eta \approx 0.3-0.4$ ). The ion absorption at low  $X[^3\text{He}]$  (as currently proposed for ITER) is very small and the total heating efficiency is only about  $\eta \approx 0.2$  in these conditions.

As mentioned, the modest RF heating efficiencies obtained in both scenarios (compared to typical heating efficiencies of  $\eta \geq 0.8$  observed in minority ICRF heating schemes) were anticipated: Fundamental majority ICRF heating suffers from the near-vanishing values of the left-hand polarized RF electric field component close to the ion cyclotron resonance layer whilst second harmonic heating scenarios typically require large fractions of the minority species to produce efficient bulk plasma heating. Despite the low efficiencies of these heating schemes, fast H ions up to 50keV and fast  $^3\text{He}$  ions up to 200keV were detected by the Neutral Particle Analyser (NPA) diagnostics in the  $N=1$  H and in the  $N=2$   $^3\text{He}$  heating experiments, respectively, when 5MW of RF power was applied. An important consequence of the low ICRF absorptivity of these heating scenarios is the enhancement of plasma-wall interactions leading to relatively large impurity content and considerable radiation losses. This is depicted in Fig.2 (left), where the total radiated power is shown as function of the ICRF power applied for the  $N = 1$  H (circles) and for the  $N = 2$   $^3\text{He}$  (triangles) heating experiments. The data correspond to 0.4s time averaged values sampled throughout the pulses. The density, temperature and NBI power ( $\sim 1.3\text{MW}$ ) were similar in all the time intervals considered.

The fact that the radiation losses for a given ICRF power level are higher for the  $N = 2$   $^3\text{He}$  case than for the fundamental H majority case is not only due to the presence of relatively large fractions of  $^3\text{He}$  in the plasma (higher  $Z_{\text{eff}}$ ), but is also related to a stronger RF-induced plasma-wall interaction observed in this case, leading to a higher impurity content in the plasma. This is depicted in Fig.2 (right), where the line emission intensity of Beryllium measured by visible spectroscopy is shown as function of the ICRF power for the two scenarios. The same time intervals as on the left figure were considered. A similar study for the  $\text{C}^{+6}$  and  $\text{C}^{+4}$  spectroscopy measurements (not shown) supported by 2D bolometer tomography indicates that most of the additional radiation observed in the  $N = 2$   $^3\text{He}$  case comes from the plasma edge and the divertor region rather than from the bulk plasma [9].

The stronger plasma wall interaction observed in the  $N = 2$   $^3\text{He}$ -H case with respect to the fundamental H majority case despite the similar ICRF heating efficiencies (and similar antenna coupling conditions) is believed not only to be related to the different RF sheath rectification effects at the two distinct RF frequencies but also to enhanced fast ion losses observed in the  $N=2$   $^3\text{He}$ -H experiments [10].

## PRELIMINARY NUMERICAL SIMULATIONS FOR ITER

Numerical simulations of the ICRF scenarios proposed for ITER's initial operation phase were performed at  $B_0 = 2.65\text{T}$  ( $I_p = 7.5\text{MA}$ ), with  $f = 42\text{MHz}$  for the H majority and H- $^4\text{He}$  scenarios and  $f = 53\text{MHz}$  for the N=2  $^3\text{He}$ -H case. The equilibrium profiles computed for 41.5MW of NBI+ECRF + ICRF auxiliary power [1] (L-mode 2:  $n_0 = 3.3 \times 10^{19} \text{ m}^{-3}$ ,  $T_i = 8\text{keV}$ ,  $T_e = 10\text{keV}$ ) were adopted in the calculations and parametric scans on plasma density, temperature and 'minority' concentration were done to assess their impact on the ICRF absorptivity of the various heating scenarios. For this study, we mainly focus on the results obtained with the 1D TOMCAT code [11], since it provides the absorbed power fraction  $\mu$  of the waves in a single-pass through the plasma (SPA). Although the SPA is closely related to the heating efficiency ( $\eta$ ) of a given ICRH scenario, a quantitative relationship between these two quantities requires a multi-pass wave model that includes power losses outside the bulk plasma (SOL, PFC's, divertor, etc.) which is outside the scope of the present paper. In practice, as long as the SPA values are not too low ( $\mu > 0.5$ ), they give a good indication of the heating efficiency observed experimentally in typical L-mode JET discharges [12]. A more detailed analysis of these heating schemes comparing the results of various 2D wave codes is reported in [3].

In figure 3, examples of the power absorption profiles obtained for the N = 1 H (left) and for the N = 2  $^3\text{He}$  (right) heating schemes in H plasmas with the 1D TOMCAT code using the plasma parameters mentioned above [1] are depicted. The dominant toroidal mode ( $n_\phi = 34$ ) of the ITER antenna spectrum with  $0\pi\pi 0$  phasing was adopted [13] and 4% of  $^3\text{He}$  was considered in the N = 2  $^3\text{He}$  heating simulations (right).

It is clear that in both cases direct fast-wave electron heating is the dominant absorption process and that the minority species in the N = 2  $^3\text{He}$  heating scheme only absorbs a very small amount of the total power at these low concentrations (as will be shown later the ion absorption is gradually enhanced by increasing  $X[^3\text{He}]$ ). Also note that parasitic absorption of H ions is possible at the high-field side in this scenario, particularly if high energy H-beams would be used. In the conditions of Fig.3, the single-pass absorption of the ICRF power is only about  $\mu = 0.3$  for the N = 1 H heating scheme (left) and about  $\mu = 0.25$  for the N = 2  $^3\text{He}$  heating scenario (right).

In figure 4 the single-pass absorption of the individual plasma species in the N = 1 H majority heating scenario plotted as function of the H temperature (left) and of the plasma central density (right) are illustrated.

By increasing the H temperature, the ion absorption is strongly enhanced due to the Doppler-shift broadening of the H cyclotron resonance layer. At  $T_H \approx 20\text{keV}$ , the ion absorption becomes dominant (the electron temperature was kept constant at  $T_e = 10\text{keV}$  in these simulations). The increase in the plasma central density leads to a strong enhancement of the total single-pass absorption, mainly due to more efficient (fast wave) electron heating. In Fig.5 the single-pass absorption of the plasma species for the N = 2  $^3\text{He}$  heating scheme is plotted as function of the  $^3\text{He}$  concentration (left) and as function of the plasma central density (right). As expected by simple theory (and as observed in



the JET experiments), the  $^3\text{He}$  absorption is gradually increased when the fraction of  $^3\text{He}$  ions is larger in the plasma while the electron absorption is virtually insensitive to the  $^3\text{He}$  concentration. However, for the ITER conditions - where the (LFS) fast wave electron absorption always plays a considerable role in the RF power balance - the  $^3\text{He}$  power absorption is practically negligible at low concentrations and one would need as much as  $X[^3\text{He}] \approx 30\%$  in the plasma to achieve dominant ion heating. The dependence of the power absorption with the plasma density is similar to the one obtained for the  $N=1$  H heating case, showing a strong increase when the central density is augmented but mainly due to enhanced electron heating. For the  $N=2$   $^3\text{He}$  heating scenario, the ICRF absorption dependence on the  $^3\text{He}$  temperature is weak.

In contrast to the two ICRF scenarios discussed so far, the fundamental H minority heating scheme to be used in the  $^4\text{He}$  plasma phase at half-field is expected to be very efficient, as long as the Hydrogen concentration in the plasma does not become too large. Examples of the power absorption profiles computed with the TOMCAT code for the H- $^4\text{He}$  heating scheme in ITER's half-field conditions for  $X[\text{H}]=5\%$  (left) and  $X[\text{H}]=30\%$  (right) are given in Fig.6. The total single-pass absorptions are  $\mu \approx 1$  and  $\mu = 0.7$ , respectively, confirming the good performance of this scenario even in the high minority concentration case, were the ion absorption is clearly jeopardized.

It is worth mentioning that the increased electron absorption observed for larger  $X[\text{H}]$  in all the simulations are not due to mode-conversion effects but rather due to an enhancement of the parallel RF field component at higher concentrations and thus more efficient fast wave Landau damping and TTMP.

The impact of the H concentration on the absorptivity of this heating scheme is illustrated in more detail in Fig.7, where the single-pass absorption per species is plotted as function of  $X[\text{H}]$  for 3 cases: (left) Reference case (L-mode 2) with  $T_e/T_i = 8/10\text{keV}$  and  $n_\phi = 34$  ( $0\pi\pi 0$ ); (centre) L-mode 1 scenario with  $T_e/T_i = 4/5\text{keV}$  and  $n_\phi = 34$  ( $0\pi\pi 0$ ); (right) L-mode 1 scenario with  $n_\phi = 60$  ( $0\pi 0\pi$ ). One sees that the H minority absorption decreases strongly with  $X[\text{H}]$  in all cases, as consequence of the less favorable RF field polarization near the IC resonance layer when the  $^4\text{He}$  plasma is diluted ('screening effect'). The electrons, on the other hand, do profit from the plasma dilution but not strongly enough to compensate the decrease in the ion absorptivity and thus the total single-pass absorption decreases from  $\mu \approx 1$  (for low H concentrations) to about  $\mu=0.6$  at  $X[\text{H}]=50\%$  in the reference case (left). At lower temperatures (centre), although the decrease in the ion absorption with  $X[\text{H}]$  is similar, the electrons do not profit as much from the change in the RF field polarization as in the high temperature case, and the total absorption is strongly compromised at high H concentrations. However, there are indications that by operating at phasing configurations that favor the excitation of high  $k_{//}$  modes (right), the good absorptivity can be recovered even at lower temperatures.

To conclude this section, let us remind that the results shown here were computed with a single toroidal mode  $n_\phi$ . As discussed in [14], considering only the dominant toroidal modes of a given antenna spectrum (instead of the full toroidal spectrum) is a good approximation for well absorbing

scenarios, as e.g. the  $N = 1$  H- $^4\text{He}$  minority scheme discussed here or the scenarios foreseen for the full-field operation phase of ITER. For low absorption scenarios such as those available for the H plasma phase, there is a considerable fraction of reactive RF power sloshing around the machine and the results are much more sensitive to the actual antenna spectrum considered.

## SUMMARY

The ICRF heating schemes proposed for ITER's half-field phase were examined. Unlike the standard H minority heating scenario foreseen for the operation in  $^4\text{He}$  plasmas, which has high single-pass absorptivity and thus is expected to yield good heating performance, it was found - both via simulations and experimentally in JET - that the heating schemes available for the H plasma operation have poor heating efficiency for the typical plasma parameters expected in the initial ITER phase. The simulations have shown that direct fast wave electron heating will dominate in both the fundamental H majority and in the 2<sup>nd</sup> harmonic  $^3\text{He}$  ICRF heating schemes, particularly at the rather modest densities and temperatures expected in the L-mode plasmas. Increased plasma density and temperature both help to enhance the ICRF power absorption but in general electron rather than ion damping is primarily improved. For the fundamental H majority heating case, the ion temperature plays a major role on the scenario's performance but ion temperatures of about 20keV are necessary to achieve dominant ion heating. For the  $N=2$   $^3\text{He}$  ICRF heating case, the ion temperature has a weaker influence and the  $^3\text{He}$  concentration is the main actuator on the heating performance. However, the simulations indicate that  $^3\text{He}$  concentrations as high as 30% are needed to achieve prevailing ion heating, with a total single-pass absorption of  $\mu \approx 0.45$ . The absorptivity is only about  $\mu \approx 0.25$  for the  $X[^3\text{He}] = 4\%$  value, presently the maximal concentration foreseen to be used in ITER.

For the half-field  $^4\text{He}$  plasma phase, the simulations indicate that fundamental H minority heating is indeed expected to be very efficient at moderate H concentrations. At higher H concentrations, there is a clear degradation in the ion absorption and the total single-pass absorption decreases. At lower temperatures (as those expected in the plasmas without ICRF), this degradation is more severe and the single-pass absorption may be as low as  $\mu = 0.3$  for  $X[\text{H}] \approx 40\%$ . This deleterious effect can, however, be compensated by operating with higher  $k_{\parallel}$  phasing configurations (as e.g.  $0\pi 0\pi$ ), at the cost of a somewhat lower antenna coupling. In general, the simulations of the half-field scenarios suggest that operating at higher  $k_{\parallel}$  phasing configurations helps to increase the total absorption, both due to a broadening of the ion-cyclotron absorption region and due to enhanced FWLD/TTMP electron damping.

Finally, it is important to mention that all the ICRF scenarios presented benefit from higher bulk plasma temperatures and therefore it is very important to assure a sufficient pre-heating of the plasma in the initial operation phase of ITER, with additional use of simultaneous NBI and ECRH auxiliary power.

## ACKNOWLEDGEMENTS

The authors would like to thank Dr. P. Lamalle and Dr. A. Loarte for the discussions on the initial heating scenarios foreseen for ITER. This work was supported by EURATOM and carried out within the framework of the European Fusion Development Agreement. The views and opinions expressed herein do not necessarily reflect those of the European Commission.

## REFERENCES

- [1]. A. Loarte and P. Lamalle, private communications
- [2]. E. Lerche *et al.*, 37<sup>th</sup> EPS Conf. on Plasma Physics, Dublin (2010), ECA **34A**, O4.121
- [3]. R. Budny *et al.*, submitted to *Nuclear Fusion*
- [4]. E. Lerche *et al.*, *Proc. of 23<sup>rd</sup> IAEA Fusion Energy Conference*, Daejeon (2010)
- [5]. V.P. Bhatnagar *et al* 1993 *Nuclear Fusion* **33** 83
- [6]. R. Koch *et al.*, 14<sup>th</sup> EPS Conf. on Plasma Physics, Madrid (1987), ECA **11D**, P3.924
- [7]. R. Bilato *et al.*, 33<sup>rd</sup> EPS Conf. on Plasma Physics, Rome (2006), ECA **30I**, P2.134
- [8]. E. Lerche *et al.*, *Plasma Physics and Controlled Fusion* **50** (2008) 035003
- [9]. A. Czarneka *et al.*, to appear in special TF-H issue of *Plasma Physics and Controlled Fusion*
- [10]. V. Kiptily *et al.*, to appear in special TF-H issue of *Plasma Physics and Controlled Fusion*
- [11]. D. Van Eester *et al.*, *Plasma Physics and Controlled Fusion* **40** (1998) 1949–1975
- [12]. R. Weynants, 18<sup>th</sup> Topical Conf. on RF Power in Plasmas, Gent (2009), AIP **1187**, p.3
- [13]. A. Messiaen *et al.*, *Nuclear Fusion* **50** (2010) 025026
- [14]. R. Dumont, 18<sup>th</sup> Topical Conf. on RF Power in Plasmas, Gent (2009), AIP **1187**, p.97

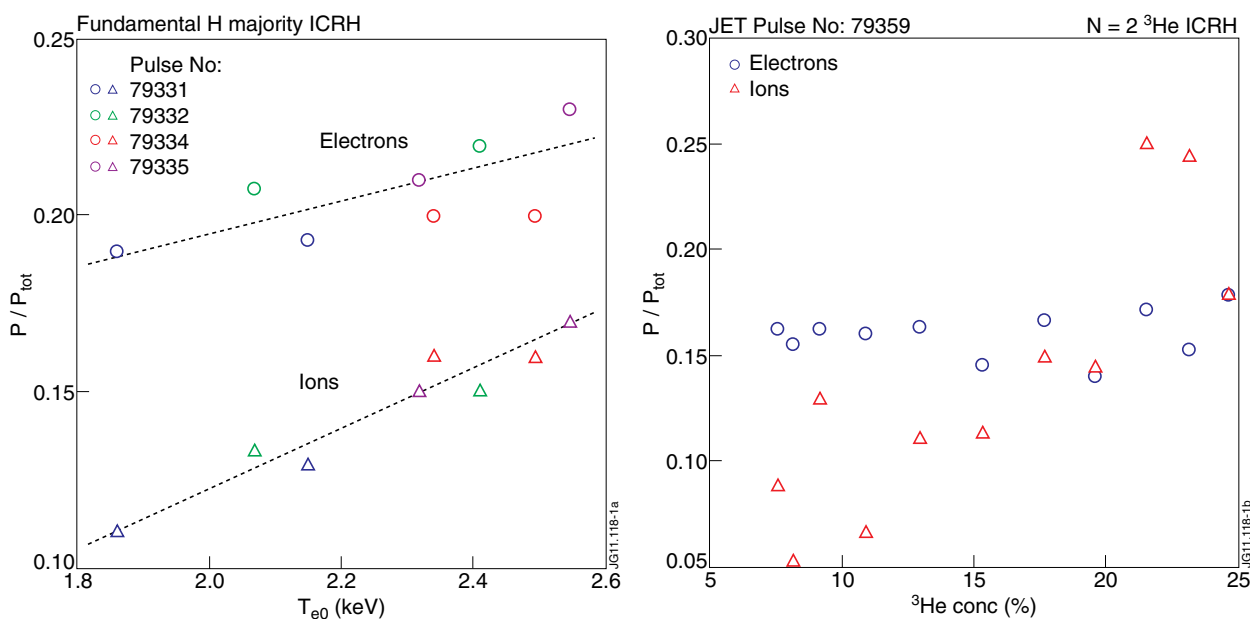


Figure 1: (Left) Ion (triangles) and electron (circles) heating efficiencies as function of the central plasma temperature for a series of discharges of the fundamental H majority ICRF scenario in JET; (Right) Ion (triangles) and electron (circles) heating efficiencies as function of the <sup>3</sup>He concentration for a discharge of the N = 2 <sup>3</sup>He ICRF heating scheme, in which a ramp-up of the <sup>3</sup>He concentration from 7-25% was imposed.

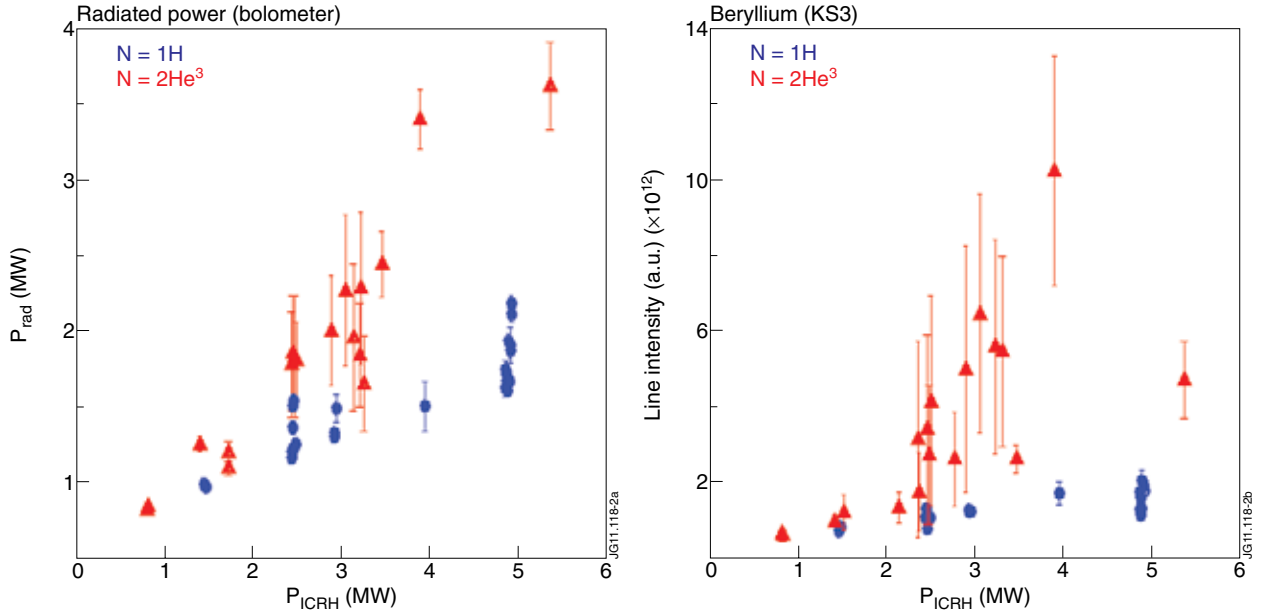


Figure 2: Total radiated power (left) and intensity of Be line (right) as function of the ICRF power for the  $N=1 H$  (circles) and the  $N=2 {}^3He$  (triangles) ICRF heating schemes.

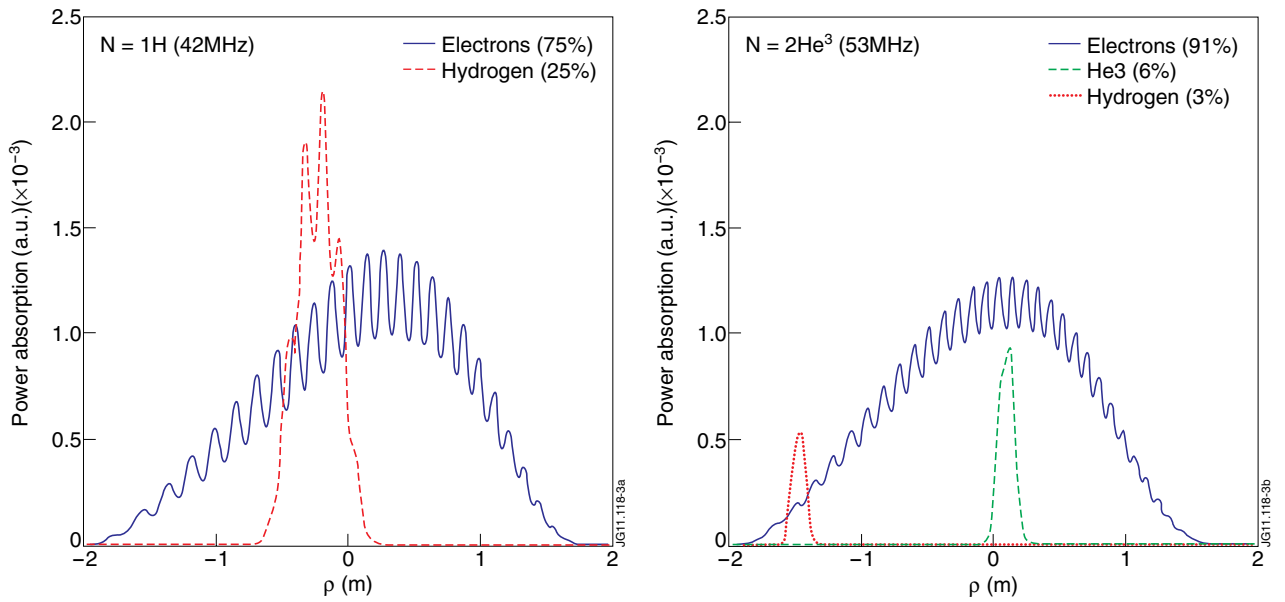


Figure 3: Power absorption profiles computed for the  $N=1 H$  (left) and for the  $N=2 {}_3He$  (right) heating scenarios for the initial ITER H plasmas at  $B_0 = 2.65T$ . For the latter, 4%  ${}^3He$  was considered in the plasma. The normalized power fractions are indicated in the legends.

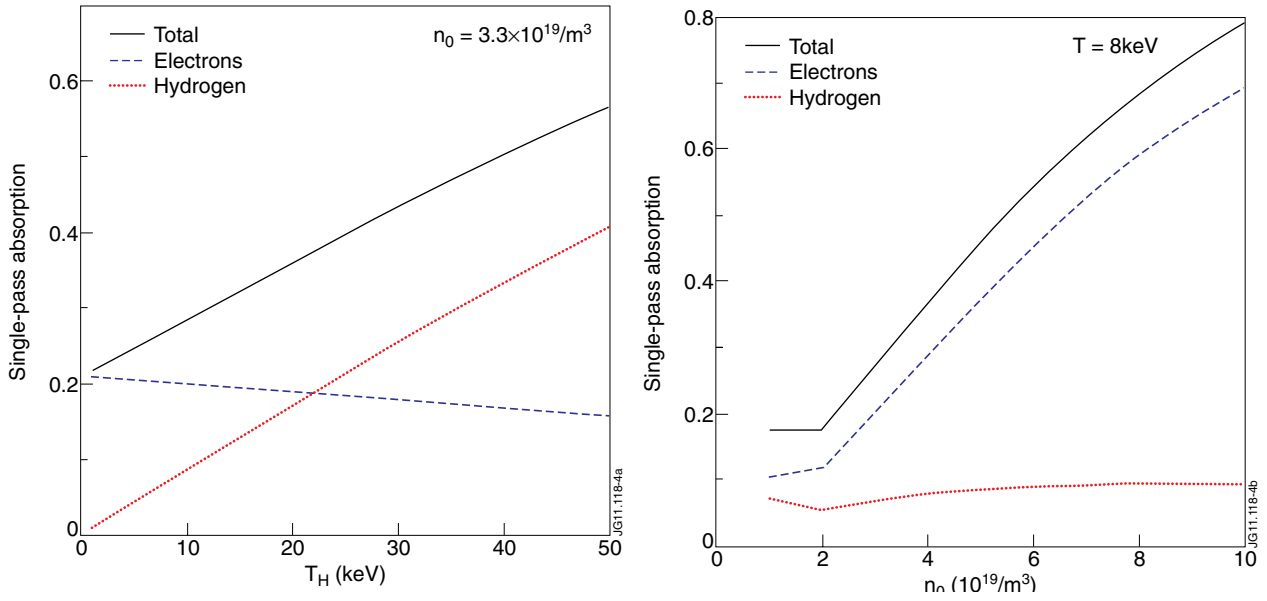


Figure 4: Dependence of the single-pass absorption of the plasma constituents as function of the Hydrogen temperature (left) and the plasma density (right) for the fundamental H majority heating scenario in ITER's half-field phase.

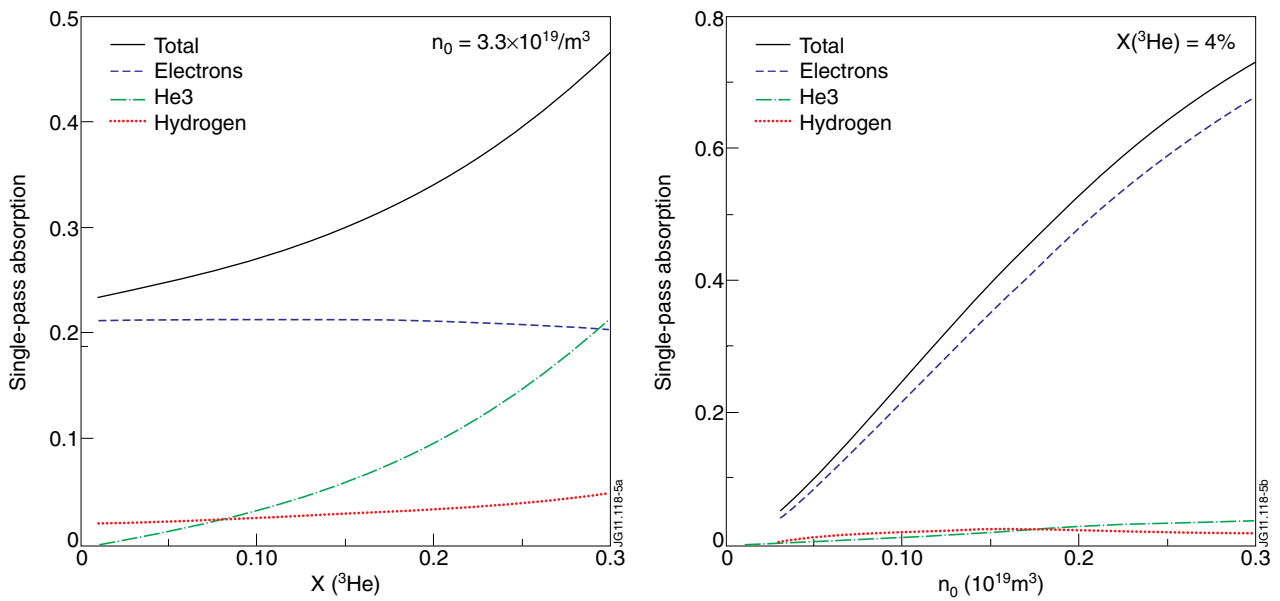


Figure 5: Dependence of the single-pass absorption on the  $^3\text{He}$  concentration (left) and on the plasma density (right) for the  $N=2$   $^3\text{He}$  heating scenario in ITER's half-field phase.

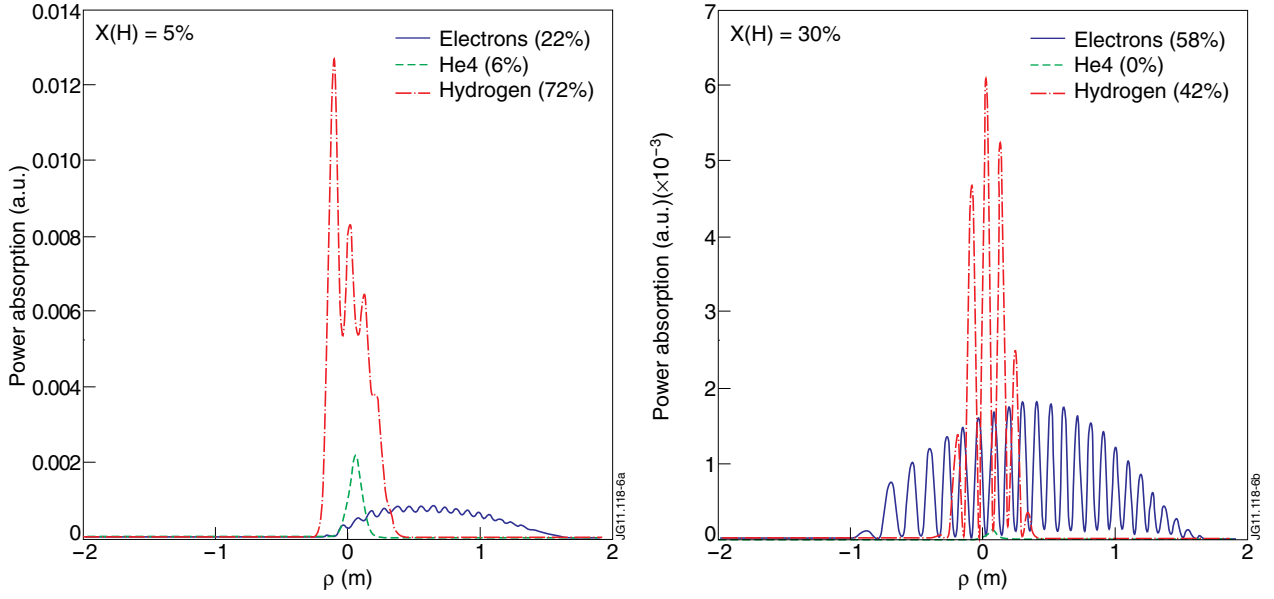


Figure 6: Power absorption profiles for the  $H\text{-}^4\text{He}$  heating scheme at  $f = 42\text{MHz}$  in the initial ITER plasma conditions for  $X[H] = 5\%$  (left) and  $X[H] = 30\%$  (right). The normalized power fractions absorbed by the various species are indicated in the legends.

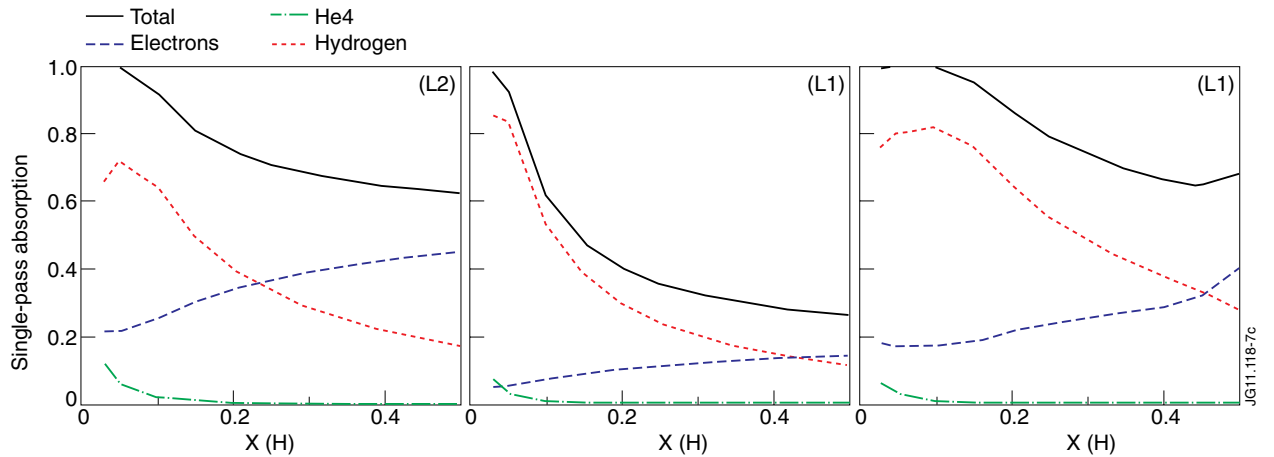


Figure 7: Single-pass absorption per species as function of  $X[H]$  for 3 different cases: (left) L-mode 2 scenario with  $T_e/T_i = 8/10\text{keV}$  and  $n_\phi = 34$  ( $0\pi\pi 0$ ); (centre) L-mode 1 scenario with  $T_e/T_i = 4/5\text{keV}$  and  $n_\phi = 34$  ( $0\pi\pi 0$ ); (right) L-mode 1 scenario with  $n_\phi = 60$  ( $0\pi 0\pi$ ).